

Acute Demyelination Disrupts the Molecular Organization of Peripheral Nervous System Nodes

EDGARDO J. ARROYO,* ERICH E. SIRKOWSKI, ROHAN CHITALE,
AND STEVEN S. SCHERER

Department of Neurology, The University of Pennsylvania Medical Center, Philadelphia,
Pennsylvania 19104-6077

ABSTRACT

Intraneurally injected lysolecithin causes both segmental and paranodal demyelination. In demyelinated internodes, axonal components of nodes fragment and disappear, glial and axonal paranodal and juxtaparanodal proteins no longer cluster, and axonal Kv1.1/Kv1.2 K⁺ channels move from the juxtaparanodal region to appose the remaining heminodes. In paranodal demyelination, a gap separates two distinct heminodes, each of which contains the molecular components of normal nodes; paranodal and juxtaparanodal proteins are properly localized. As in normal nodes, widened nodal regions contain little or no band 4.1B. Lysolecithin also causes “unwinding” of paranodes: The spiral of Schwann cell membrane moves away from the paranodes, but the glial and axonal components of septate-like junctions remain colocalized. Thus, acute demyelination has distinct effects on the molecular organization of the nodal, paranodal, and juxtaparanodal region, reflecting altered axon–Schwann cell interactions. *J. Comp. Neurol.* 479:424–434, 2004. © 2004 Wiley-Liss, Inc.

Indexing terms: myelin; Schwann cells; septate-like junctions; axon–glia interactions; channels; lysolecithin

The molecular organization of the axonal membrane is highly related to that of its myelin sheaths (Rasband and Shrager, 2000; Girault and Peles, 2002; Kazarinova-Noyes and Shrager, 2002; Poliak and Peles, 2003; Scherer et al., 2004). In both the CNS and the PNS, the nodal membrane contains high concentrations of voltage-gated Na⁺ (Na_v) channels, the K⁺ channel KCNQ2, neurofascin 186 (NF186), and NrCAM, all linked to the spectrin cytoskeleton by ankyrin_G. The paranodal region is distinguished by septate-like junctions that link the axonal membrane to the spiral of glial endfeet. Contactin and contactin-associated protein (Caspr; also known as “paranodin”) form heterodimers that are localized to the paranodal axonal membrane. An alternatively spliced isoform of neurofascin, NF155, is localized on the membrane of the glial endfeet apposing the paranodal axonal membrane, so that contactin, Caspr, and NF155 are all components of septate-like junctions. The juxtaparanodal axonal membrane contains high levels of Kv1.1 and Kv1.2 (*Shaker*-type K⁺ channels), their β subunit (Kvβ2), Caspr2 (an additional member of the Caspr family), and TAG-1; the juxtaparanodal Schwann cell membrane contains TAG-1 and connexin29 (Cx29). Axonal and glial TAG-1 interact *in trans*, thereby linking the axonal and glial juxtapara-

nodal membranes. An isoform of band 4.1 protein, band 4.1B, probably links the glycoprotein domains of Caspr and Caspr2 to the spectrin cytoskeleton in the paranodal and juxtaparanodal regions.

Most inherited dysmyelinating and demyelinating diseases that affect the PNS and/or the CNS have been linked to mutations in genes that are expressed in the myelinating cells themselves (Suter and Scherer, 2003). Although these inherited dysmyelination/demyelinating diseases are caused by cell autonomous defects in the myelinating glial cells, nonautonomous axonal damage has been increasingly implicated as an important aspect of these diseases (Griffiths et al., 1998; Martini, 2001;

Grant sponsor: The Charcot-Marie-Tooth Association (to E.J.A.); Grant sponsor: National Institutes of Health; Grant number: NS08075 (to S.S.S.); Grant number: NS34528 (to S.S.S.).

*Correspondence to: Edgardo J. Arroyo, 464 Stemmler Hall, 36th Street and Hamilton Walk, The University of Pennsylvania Medical Center, Philadelphia, PA 19104-6077. E-mail: arroyoe@mail.med.upenn.edu

Received 12 May 2004; Revised 12 August 2004; Accepted 13 August 2004

DOI 10.1002/cne.20321

Published online in Wiley InterScience (www.interscience.wiley.com).

Lappe-Siefke et al., 2003). How demyelination leads to axonal loss is not known, but the reorganization of the axonal membrane is the earliest known alteration. In the absence of myelin sheaths, erstwhile juxtaparanodal proteins (Kv1.1, Kv1.2, Kv β 2, and Caspr2) are mislocalized to the paranodal region (Rasband et al., 1998; Mathis et al., 2001; Arroyo et al., 2002; Poliak and Peles, 2003). Just disrupting the septate-like junctions, leaving the myelin sheaths otherwise intact, is sufficient to cause the mislocalization of these juxtaparanodal proteins and also results in the failure of contactin, Caspr, and NF155 to cluster (Popko, 2000; Bhat et al., 2001; Boyle et al., 2001; Mathis et al., 2001; Arroyo et al., 2002; Honke et al., 2002; Poliak and Peles, 2003). How demyelination affects the molecular components of nodes has been less well studied. Na ν channels appear to dissipate during acute demyelination and reform adjacent to myelin sheaths (Dugandzija-Novakovic et al., 1995; Novakovic et al., 1996); whether other nodal components are similarly affected remains to be determined.

In inherited dysmyelinating/demyelinating diseases, demyelination and remyelination are ongoing, coexisting even on the same myelinated fiber, resulting in a complex pathological picture. To simplify the analysis of how demyelination affects the organization of the axonal membrane, we injected lyssolecithin into rat sciatic nerves; this causes severe, focal demyelination that is promptly followed by remyelination (Hall and Gregson, 1971; Hall, 1973). Prior studies using this model showed that nodal clusters of Na ν channels and juxtaparanodal clusters of Kv1.1 and Kv1.2 channels disperse after demyelination and reorganize with remyelination (Dugandzija-Novakovic et al., 1995; Novakovic et al., 1996; Rasband et al., 1998). We find that segmental demyelination results in the simultaneous loss of multiple components of nodes, paranodes, and juxtaparanodes but that paranodal demyelination results in the spatial shifting, but not the overt loss, of these components.

MATERIALS AND METHODS

Lyssolecithin injections

Young adult Sprague-Dawley rats were anesthetized, and the sciatic nerve was exposed. We used a glass micropipette (tip diameter approximately 20 μ m) to inject 1–2 μ l of 1% lyssolecithin in Locke's solution (154 mM NaCl, 5.6 mM KCl, 2 mM CaCl $_2$, 10 mM HEPES, pH 7.4) intraneurally near the sciatic notch at 1 μ l/minute (Rasband et al., 1998). The site of injection was marked with carbon particles for identifying the lesion site. At 4, 5, 6, and 7 days postinjection (N = 10 per time point), the sciatic nerves were dissected, fixed for 30 minutes in 4% paraformaldehyde (0.1 M phosphate buffer, pH 7.4; PB), rinsed in 0.1 M PB, and teased into small bundles on SuperFrost Plus glass slides (Fisher Scientific, Pittsburgh, PA) using fine tungsten or stainless steel needles, dried overnight, and stored at –20°C.

Immunohistochemistry

Teased nerve fibers were postfixed and permeabilized by immersion in –20°C acetone for 10 minutes, blocked at room temperature for at least 1 hour in 5% fish skin gelatin containing 0.5% Triton X-100 in PBS, and incubated 24–48 hours at 4°C with various combinations of

TABLE 1. Antibodies, Dilutions, and Sources

Antibody	Dilution	Source/reference
Rabbit α pan-Na ν	1:500	Vabnick et al., 1997
Rabbit α syndecan-3	1:250	Asundi et al., 2003
Rabbit α ankyrin $_G$	1:100	Lambert et al., 1997
Rabbit α Kv1.1	1:200	Alomone Laboratory
Rabbit α Kv1.2	1:100	Alomone Laboratory
Rabbit α Caspr	1:500	Peles et al., 1997
Rabbit α protein 4.1B	1:500	Denisenko-Nehrbass et al., 2003
Rabbit α NF155 kDa	1:750	Tait et al., 2000
Rabbit α KCNQ2	1:100	Cooper et al., 2001
Rabbit α Cx29	1:300	Altevogt et al., 2002
Mouse α pan-Na ν channels	1:50	Sigma
Mouse α ankyrin $_G$	1:100	Zymed
Mouse α ezrin	1:100	Sigma
Mouse α Kv1.1	1:50	Upstate Biotechnology, Inc.
Mouse α Kv1.2	1:50	Upstate Biotechnology, Inc.
Mouse α rat MAG (513)	1:100	Boehringer Mannheim
Mouse α Caspr	1:50	Poliak et al., 1999
Mouse α Caspr	1:50	Rasband and Trimmer, 2001
Mouse α (pan-) neurofascin	1:200	Gift of Dr. Matt Rasband
Rat α NFH (Ta51)	1:10	Lee et al., 1982, 1987
Goat α protein 4.1B	1:500	Ohara et al., 2000
Chicken α spectrin β IV	1:100	Komada and Soriano, 2002

primary antibodies (Table 1) diluted in blocking solution. For the rabbit antiserum against NF155, tissues were postfixed for 1 minutes in Bouin's fixative. After being incubated with the primary antibodies, the slides were washed; incubated with the appropriate fluorescein-, rhodamine-, and cyanine-5-conjugated donkey cross-affinity purified secondary antibodies (diluted 1:100; Jackson ImmunoResearch Laboratories, West Grove, PA); counterstained with DAPI; and mounted with Vectashield (Vector Laboratories, Inc., Burlingame, CA). The slides were examined by epifluorescence with appropriate filters on a Leica DMR light microscope and photographed with a Hamamatsu digital camera using OpenLab or with a Leica TCS laser scanning confocal microscope. Images were manipulated with Adobe Photoshop.

Electron microscopy

Wild-type adult rats 5 (n = 3), 6 (n = 3), and 7 (n = 1) days postinjection (dpi) were perfused with 0.9% NaCl, followed by 3% glutaraldehyde in PB. The sciatic nerves were removed, cut into 5-mm-long segments centered on the site of injection, and fixed overnight at 4°C in the same fixative. On the next day, the sciatic nerves were washed in PB, osmicated in 1% OsO $_4$ for 1 hour at room temperature, then dehydrated in graded ethanols, infiltrated with propylene oxide then Epon, and polymerized at 60°C. Semithin sections were stained with toluidine blue; ultrathin sections were stained with lead citrate and photographed with a Zeiss EM10 electron microscope. Electron micrographs were printed and scanned; these images were imported into Adobe Photoshop and assembled.

Statistical analysis

We counted affected fibers from lyssolecithin-treated rats and classified such fibers with regard to their level of demyelination and the morphology of their paranodes, as shown in Table 2. Teased fibers from sciatic nerves at 5 (n = 3), 6 (n = 3), and 7 (n = 3) dpi were immunostained with Rb α Caspr, M α PanNa ν , and Rat α NF-H. An analysis of variance (ANOVA) was used to assess whether the number of affected fibers obtained at 5 dpi was different from that at 7 dpi.

TABLE 2. Changing Paranodal Pathologies 5–7 dpi¹

	5 dpi (%; n=3)	6 dpi (%; n=3)	7 dpi (%; n=3)	5 vs. 7 dpi ANOVA (P)
1	4	5	3	0.16
2	2	0	1	
3	37	43	14	
4	13	15	5	0.10
5	3	2	5	
6	34	25	58	
7	7	10	15	
Affected nodes counted	166	81	266	

¹Teased fibers at 5, 6, and 7 dpi were immunostained for Caspr. Fibers with one of the depicted pathological changes were counted; the mean percentage is shown at each dpi. Arrowheads depict the positions of nodes; the squares depict intact paranodes; vertical lines depict “unwound” paranodes; no paranodes depict demyelinated internodes. Abnormally widened nodes were more than 5 μm in width, whereas normal nodes are 1–2 μm wide. Between 5 and 7 dpi, the proportion of fibers with paranodal demyelination (groups 3–5) decreases, whereas the proportion of fibers with segmental demyelination (groups 6 and 7) increases, but without reaching statistical significance. The total percentage of unwound profiles at each time point is shown below.

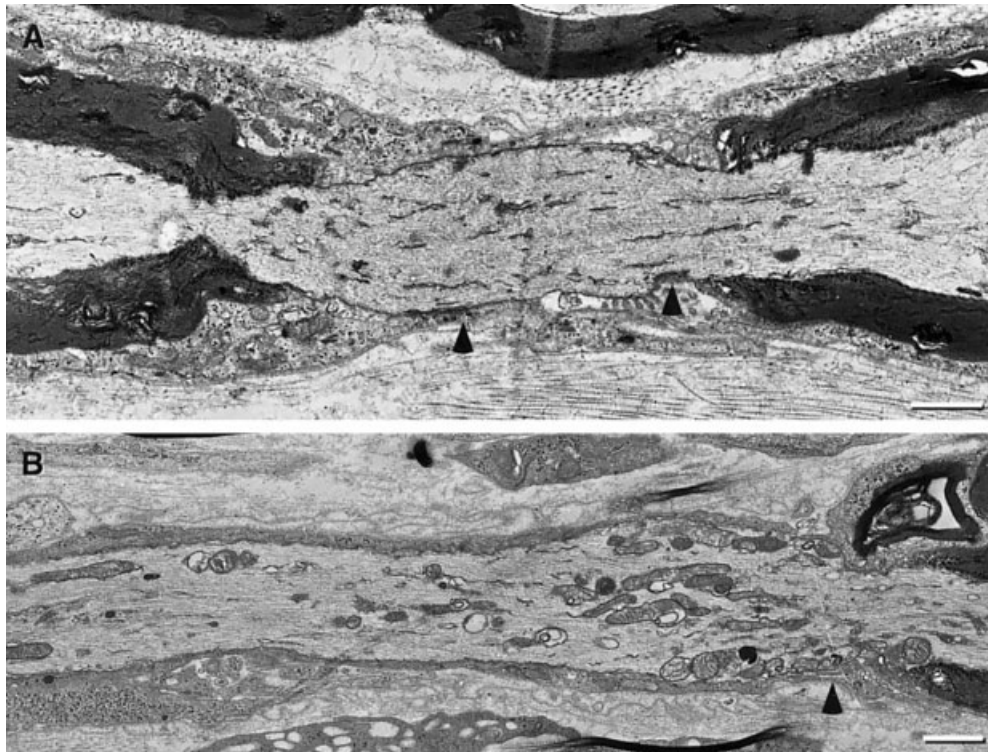


Fig 1. Fine structure of paranodal and segmental demyelination. These are electron micrographs of longitudinally sectioned nerves. **A** (6 dpi) and **B** (7 dpi) show examples of paranodal and segmental demyelination, respectively. Arrowheads indicate the location of heminodes. Scale bars = 1 μm.

RESULTS

Lysolecithin causes paranodal and segmental demyelination: ultrastructural analysis

To reinvestigate the consequences of lysolecithin (Hall and Gregson, 1971; Hall, 1973), we examined longitudinal

sections of the injected region by electron microscopy. At 5–7 dpi, there were many large axons ensheathed but not myelinated by cellular processes; these are “demyelinated” axons. Some of these demyelinated axons were in continuity with myelinated axons, demonstrating the segmental nature of demyelination (Fig. 1B). A “heminode” marks the site of transition between the myelinated and

the demyelinated regions. We also noted abnormally widened nodes flanked on both sides by paranodes; these are examples of what has been termed “paranodal demyelination” (Fig. 1A). Two “heminodes” flank these widened nodes.

Paranodal and segmental demyelination alter the molecular organization of nodes

To determine how acute demyelination affects the organization of the axonal membrane, we immunostained teased fibers from the injected region with combinations of antibodies against various components of the nodal region (Table 1). As previously reported (Hall and Gregson, 1971; Rasband et al., 1998), few myelinated fibers were affected at 4 dpi, but many fibers were affected between 5 and 7 dpi. Figure 2A shows an example of a normal-appearing myelinated axon, immunostained for neurofilament heavy (NF-H), Caspr, and myelin-associated glycoprotein (MAG). MAG is prominently expressed in the paranodal region and serves to demarcate the extent of the myelin sheath. The node itself has diminished staining for a monoclonal antibody that recognizes a phosphorylated epitope of NF-H (Lee et al., 1982, 1987; Mata et al., 1992; Arroyo et al., 1999) and is flanked by Caspr-positive paranodes.

Between 5 and 7 dpi, many fibers showed paranodal demyelination. Figure 2B shows an example, a widened axonal segment flanked on both sides by Caspr- and MAG-positive paranodes. NF-H staining was present in these widened axonal segments but often diminished immediately adjacent to each paranode, so that each paranode appeared to be associated with a heminode (see below). Some widened segments were up to 50 μm long (Fig. 2C). Both demyelinated paranodes and segmentally demyelinated axons lacked MAG staining, but segmentally demyelinated axons were longer and had multiple associated nuclei (compare Fig. 2C and D).

Heminodes have the molecular components of nodes

To determine whether paranodally and segmentally demyelinated axons had nodal specializations, we immunostained the axonal and glial components of nodes. Compared with normal myelinated axons (Fig. 3A), paranodal demyelination appeared to “split” the original node into two heminodes, each of which remained associated with its respective paranode. As with nodes, these heminodes contained Na_V channels (Fig. 3B,C), ankyrin_G (Fig. 3D,E), spectrin βIV (Fig. 3F–I), NF186 (Fig. 3H,I), and KCNQ2 (data not shown). Similarly, heminodes adjacent to segmentally demyelinated internodes also remained intact, as demonstrated by preserved staining for Na_V channels, ankyrin_G, spectrin βIV , NF186 (Fig. 3C,E,G,I), and KCNQ2 (data not shown). In contrast, the other heminode (formerly associated with the now demyelinated internode) appeared to fragment: Small clusters of Na_V channels (Fig. 3C), ankyrin_G (Fig. 3E), and spectrin βIV (Fig. 3G) and KCNQ2 (data not shown) immunoreactivity were dispersed in the region immediately adjacent to the intact heminode.

To determine whether nodal Schwann cell microvilli appose heminodes, we immunostained for ezrin (Melendez-Vasquez et al., 2001; Scherer et al., 2001), syndecan-3 (Goutebroze et al., 2003), and NF155 (although NF155 is much more prominent at paranodes; Brown et al., 2001). Ezrin was localized to Schwann cell

membranes at heminodes associated with paranodal (Fig. 4A) or segmental demyelination (Fig. 4B). We made similar observations for syndecan-3 and NF155 (data not shown), although the latter stained inconsistently. Some fragments of ankyrin_G immunoreactivity in demyelinated regions were apposed by ezrin immunoreactivity (Fig. 4B). These data indicate that “nodally specialized” Schwann cell and axonal membranes remain apposed even under pathological conditions.

“Unwound” paranodes

As shown in Figure 3A, normal paranodes separate juxtaparanodal Kv1.1/Kv1.2 channels from nodal Na_V channels. In segmentally demyelinated fibers, however, Kv1.1/Kv1.2 channels were concentrated in the former paranode (Fig. 3C, † to the right of the Na_V staining), abutting the node (Rasband et al., 1998). Kv1.1/Kv1.2 channels were also aberrantly localized to some paranodes associated with paranodal demyelination (Fig. 3B; † to the right of the right heminode), indicating that these paranodes incompletely sequester juxtaparanodal proteins. To investigate this issue further, we compared the localization of Caspr and NF155, two components of septate-like junctions. Caspr and NF155 were colocalized at all paranodes, normal-appearing ones as well as those associated with segmental or paranodal demyelination (Fig. 5). Some paranodes (about 30% of abnormal fibers at each time point; Table 2), furthermore, appeared to be “unwound” (Fig. 5C). By unwound, we mean that there were gaps between the spirals of Caspr/NF155 staining in the paranodal region and that the spiral of Caspr/NF155 staining extended beyond the paranode region, into the internode (Figs. 5C, 6F). These unwound paranodes, furthermore, did not exclude Kv1.2 channels from the paranodal region (Figs. 3B, 6F).

Altered Schwann cell juxtaparanodes

To investigate whether the juxtaparanodal proteins of the Schwann cell myelin sheath are affected by segmental and paranodal demyelination, we immunostained teased fibers for Cx29, which is localized by the juxtaparanodal Schwann cell membrane (Altevogt et al., 2002; Li et al., 2002). Schwann cells associated with segmentally demyelinated fibers had no Cx29 immunostaining (Fig. 6A). In paranodal demyelination, Cx29 remains associated with the juxtaparanodal region; it is not found in the gap between the heminodes (Fig. 6B).

Redistribution of protein 4.1B in demyelinated regions

As shown in Figure 6C, protein 4.1B is highly enriched at paranodes (more than juxtaparanodes and internodes) but appears to be absent at nodes (Menegoz et al., 1997; Poliak et al., 1999; Ohara et al., 2000; Parra et al., 2000; Denisenko-Nehrbass et al., 2003). The abnormally widened nodal regions in paranodal demyelination (Fig. 6D) and the demyelinated internodes (Fig. 6E) also had markedly diminished protein 4.1B. Protein 4.1B still appears to be colocalized with Caspr in the paranodal region (Fig. 6E) and even with “unwound strands” of Caspr (data not shown). In contrast to normal-appearing myelinated fibers (Fig. 6C), the relative amount of paranodal and juxtaparanodal protein 4.1B tended to be similar in myelinated axons that were adjacent to demyelinated internodes or

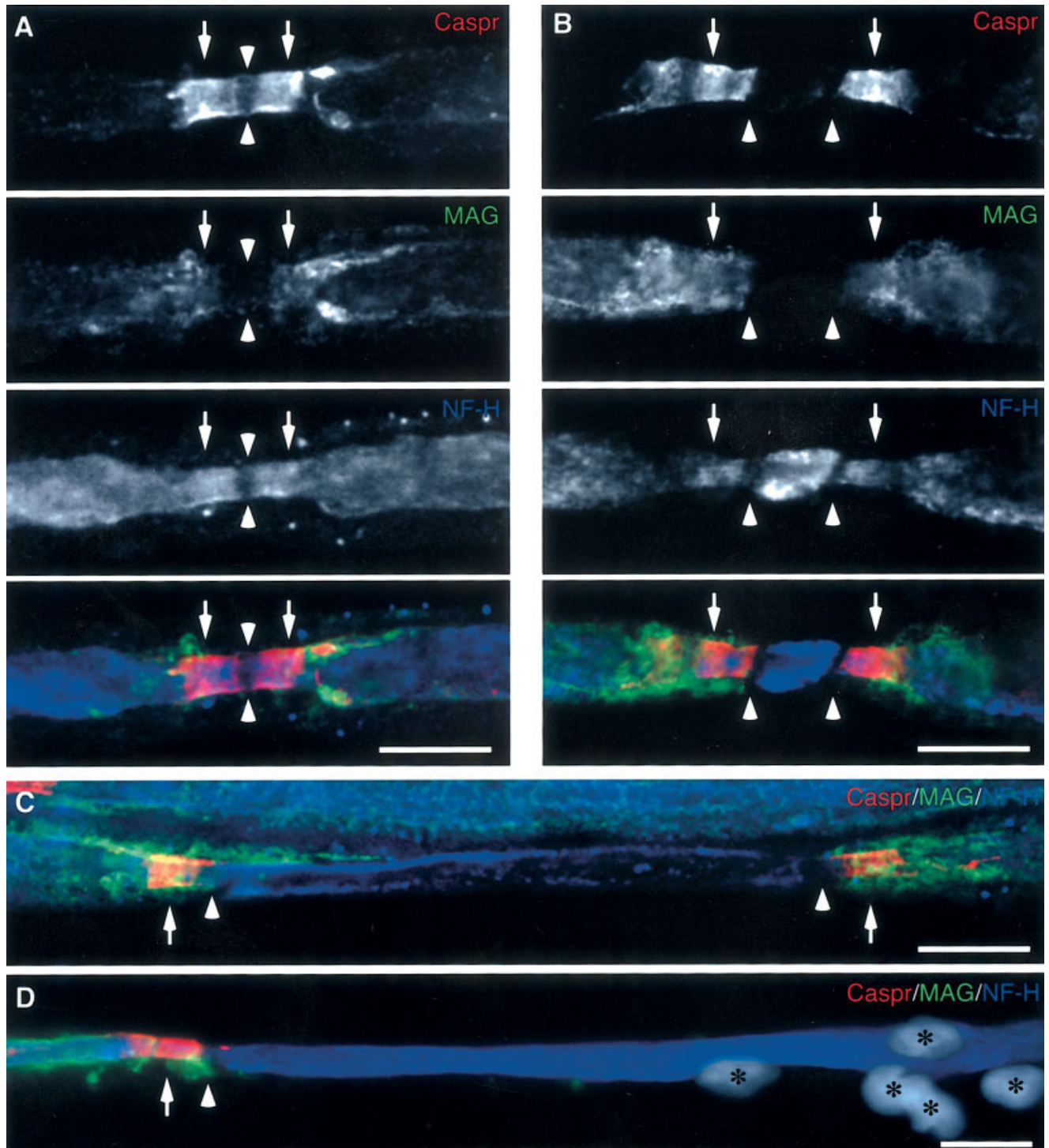


Fig. 2. Lysolecithin causes paranodal and segmental demyelination. These are images of teased fibers 5–7 dpi, immunolabeled as indicated. **A** shows a normal appearing node, **B** and **C** are examples of paranodal demyelination, and **D** is an example of segmental demyelination. Apposed pairs of arrowheads indicate the locations of nodes, single arrowheads indicate the locations of heminodes, arrows indi-

cate the locations of paranodes, and asterisks denote DAPI-stained nuclei (gray). In **B** and **C**, note that the widened nodal region is NF-H-positive but MAG- and Caspr-negative. In **D**, note the nuclei that are associated with the demyelinated internode. Scale bars = 10 μ m.

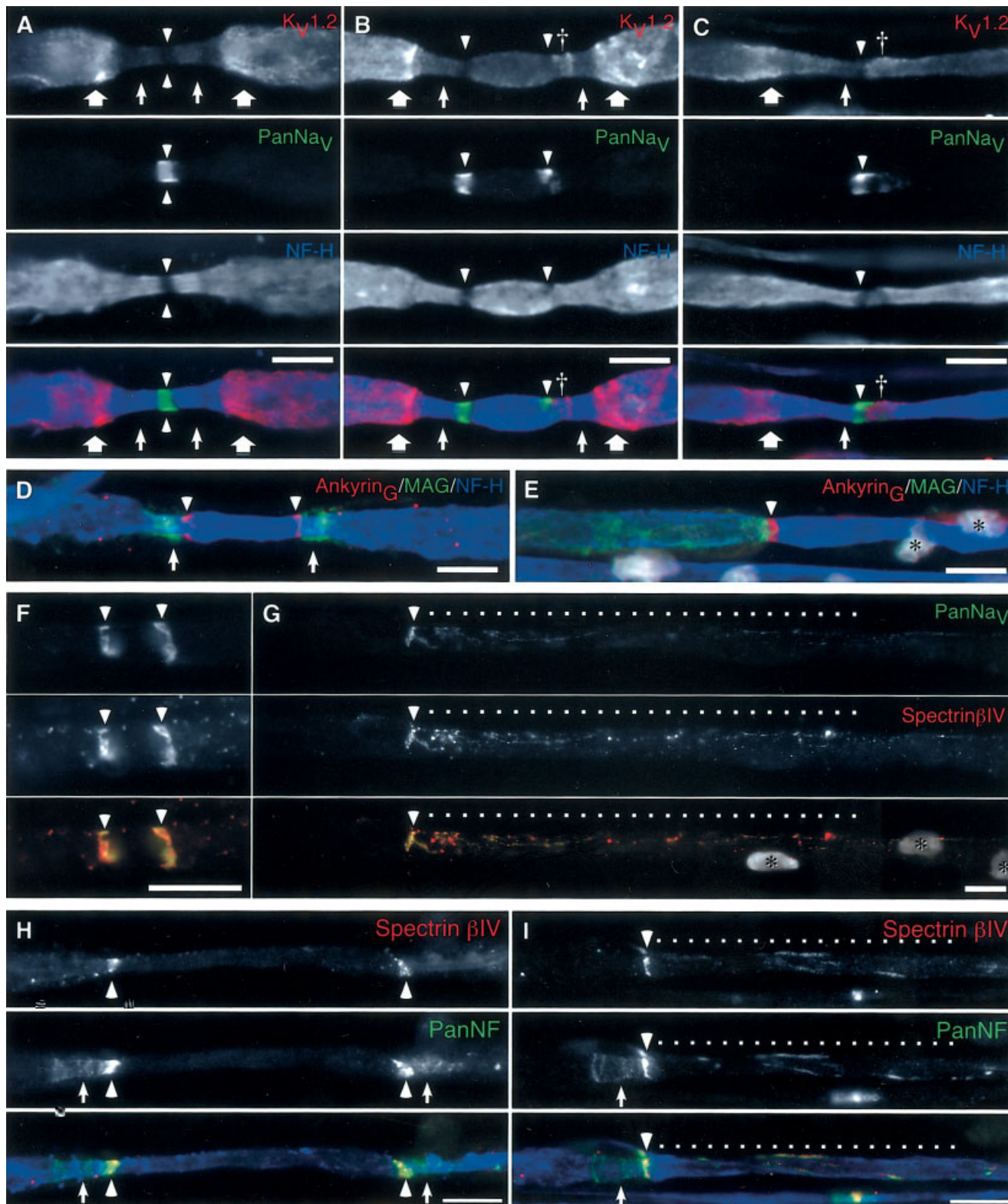


Fig. 3. Paranodal and segmental demyelination disrupts axonal components of nodes. These are images of teased fibers 5–7 dpi, immunolabeled as indicated. **A** shows a normal-appearing node; **B**, **D**, **F**, and **H** are examples of paranodal demyelination; and **C**, **E**, **G**, and **I** are examples of segmental demyelination. The pan-NF monoclonal antibody recognizes both glial/NF155 and axonal/NF186 isoforms (Tait et al., 2000). Thick arrows mark juxtapanodes; other symbols are as in Figure 2. Note that each heminode contains the

axonal components of nodes (Na_v channels, ankyrin_G, spectrin βIV, and neurofascin; pan-NF); that Kv1.2 apposes nodal Na_v channels in paranodally (**B**) and segmentally (**C**) demyelinated axons (marked by †); and that Na_v channels, spectrin βIV, and neurofascin (dots in **C**, **G**, **I**) are dispersed along demyelinated internodes, which can be recognized by their lack of MAG staining and/or their associated Schwann cell nuclei (asterisks; not shown in **C**). Scale bars = 10 μm.

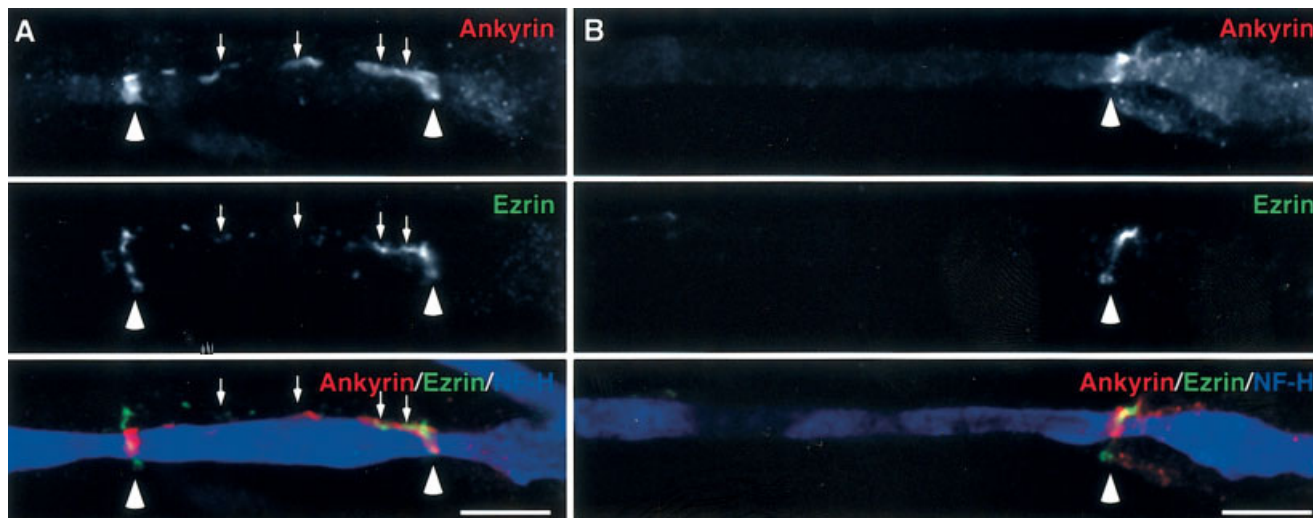


Fig. 4. Schwann cell processes are associated with heminodes. These are images of teased fibers 5–7 dpi, immunolabeled as indicated. Ezrin-positive Schwann cell processes appose ankyrin_C-positive heminodes formed by paranodal (A) or segmental (B) demyelination (arrowheads). Note patches of ezrin and ankyrin_C in a demyelinated region (arrows in A). Scale bars = 10 μ m.

were themselves affected (Fig. 6D,E). These data support, but do not themselves directly demonstrate, a role for Caspr and Caspr2 in localizing protein 4.1B in myelinated axons.

Quantitative analysis

To evaluate the relative frequency of pathologically affected nodes, we classified and counted abnormal nodes from teased fibers that were immunostained for Caspr (Table 2). We classified abnormal nodes according to the presence of segmental or paranodal demyelination and the integrity of the paranode (normal or “unwound”). Because it was not possible to relate the number of pathological nodes to the total number of nodes, we compared the relative frequencies of abnormal nodes themselves. This analysis showed that paranodal demyelination was more common at 5 than at 7dpi ($P = 0.16$, ANOVA). Conversely, segmentally demyelinated axons were more common at 7 dpi than at 5 dpi ($P = 0.10$, ANOVA). Taken together, these data raise the possibility that paranodal demyelination leads to segmental demyelination.

DISCUSSION

Intraneural injection of lyssolecithin causes segmental and paranodal demyelination as well as “unwound” paranodes. In each kind of pathological alteration, axonal proteins are redistributed in relation to the molecular specializations of Schwann cells. Specialized (ezrin-positive) Schwann cell processes are associated with heminodes, which appear to retain the complete ensemble of axonal components. Even in fragmented nodes, Schwann cell processes and axonal molecular components may be found together. Similarly, Caspr and NF155 remain colocalized; this is particularly striking in unwound paranodes. Finally, regions lacking myelin sheaths, such as demyelinated internodes and abnormally widened nodes, have reduced protein 4.1B.

These data indicate that axon–Schwann cell interactions govern the clustering of the axonal molecules that characterize the nodal, paranodal, and juxtaparanodal regions. That lyssolecithin directly affects the molecular organization of axonal membranes is unlikely, because systemic administration of β,β' -iminodipropionitrile produces similar changes in the axonal organization (Nguyen et al., 2004).

Molecular reorganization accompanying segmental demyelination

Intraneural injection of lyssolecithin produces predominantly segmental demyelination, with little if any axonal loss (Hall and Gregson, 1971; Hall, 1973). As noted previously, the onset of demyelination occurs at about 4 dpi, and demyelination becomes more pronounced over the next few days. In agreement with previous reports, we find that Na_v channels disperse after segmental demyelination, allowing Kv1.1/Kv1.2 channels to abut nodes (Dugandzija-Novakovic et al., 1995; Novakovic et al., 1996; Rasband et al., 1998). We have confirmed and extended these findings by showing that other nodal components (ankyrin_C, spectrin β IV, NF186, and KCNQ2) remain associated with Na_v channels, that specialized (ezrin- and syndecan-3-positive) Schwann cell processes remain localized to heminodes and even nodal fragments, that protein 4.1B is markedly diminished in demyelinated regions, and that the abnormally localized Kv1.1/Kv1.2 channels (adjacent to nodes) are associated with the loss of paranodal Caspr and NF155. Thus, demyelinated PNS internodes have but a few vestiges of their original molecular organization. Comparable findings have been made in the CNS, with the possible exception that nodal clusters of Na_v channels, ankyrin_C, and KCNQ2 persist in at least one model of severe dysmyelination, the *md* rat (Arroyo et al., 2002; Devaux et al., 2003, 2004).

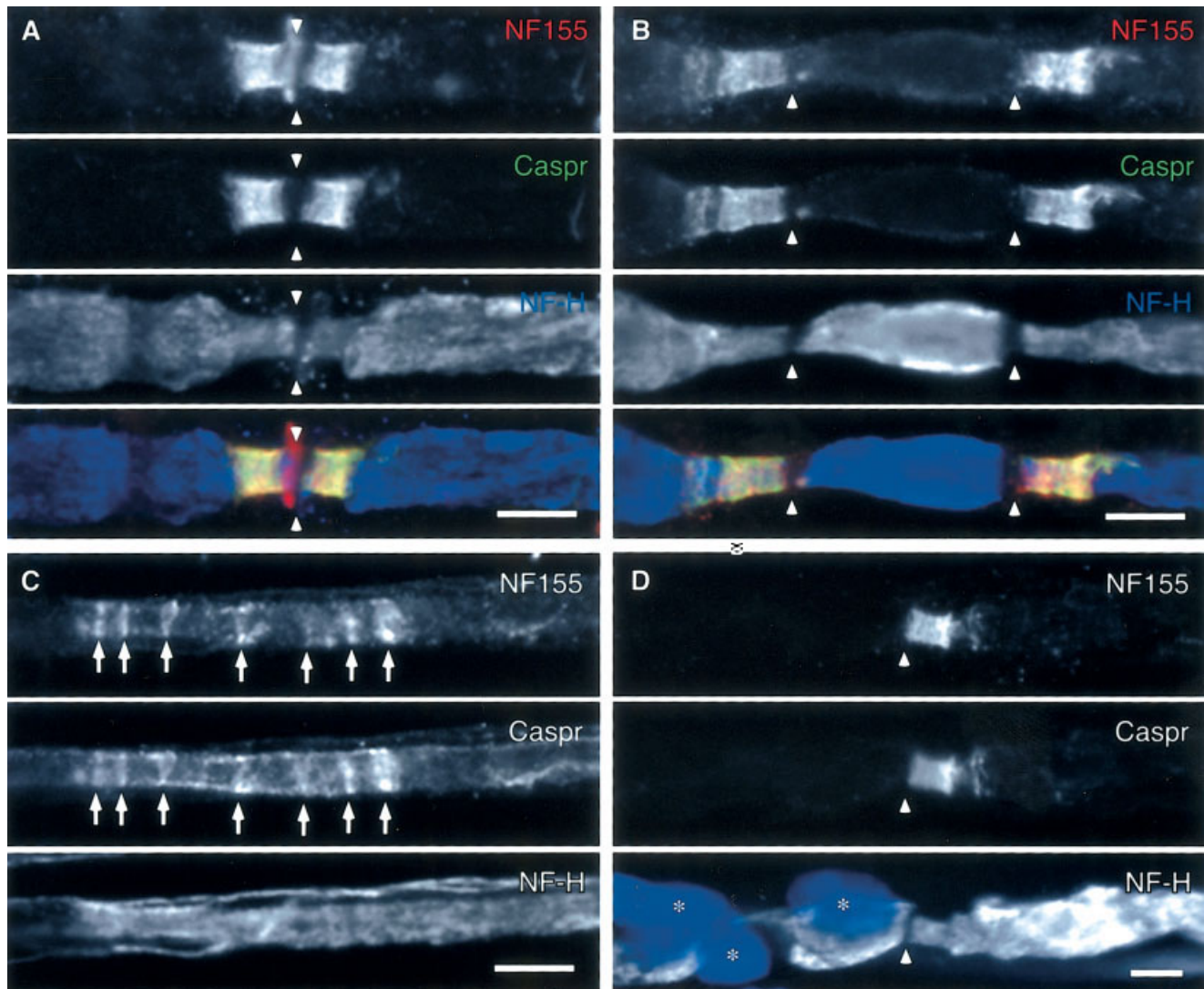


Fig. 5. Paranodal and segmental demyelination disrupts glial and axonal components of paranodes. These are images of teased fibers 5–7 dpi, immunolabeled as indicated. **A** shows a normal-appearing node, **B** an example of paranodal demyelination, **C** an example of an “unwound” paranode, and **D** is an example of segmental demyelina-

tion. Symbols are as in Figure 2, except that the small arrows in **C** indicate the spirals of the unwound paranode, and the nuclei in **D** are blue (asterisks). Note that Caspr and NF155 are colocalized in every image. Scale bars = 5 μ m.

Molecular reorganization accompanying paranodal demyelination

Whereas segmental demyelination is the chief lesion caused by lysolecithin, paranodal demyelination has been noted (Hall and Gregson, 1971; Hall, 1973). It remains to be determined whether paranodal demyelination contributes to the conduction block caused by lysolecithin injections (Smith and Hall, 1980).

Paranodal demyelination is also caused by wide variety of immune (Ballin and Thomas, 1969a,b; Allt, 1975; Bonnaud-Toulze and Raine, 1980), toxic (Allt, 1969; Jones and Cavanagh, 1983; Griffin et al., 1987), and mechanical (Lubinska, 1958; Ochoa, 1972; Foster et al., 1980; Dyck et al., 1990; Abe et al., 2002) agents. In spite of its potential importance, its only molecular attribute is that paranodal demyelination splits nodes into two heminodes of Na_V

channels (Dugandzija-Novakovic et al., 1995; Novakovic et al., 1996). We found that ankyrin_C, spectrin β IV, NF186, and KCNQ2 behave similarly and that specialized (ezrin-positive) Schwann cell processes remain associated with each heminode. Thus, these data provide further evidence that normal nodes consist of two heminodes that fuse during development (Dugandzija-Novakovic et al., 1995; Novakovic et al., 1996; Rasband et al., 1998; Ching et al., 1999), and there is evidence that heminodes formed under pathological conditions may rejoin to form nodes (Allt, 1969; Hall, 1973; Bonnaud-Toulze and Raine, 1980).

Unwound paranodes

Unwound paranodes can be conceptualized as a change in the shape on the myelin sheath, as depicted in Figure 7. They were an unexpected consequence of lysolecithin in-

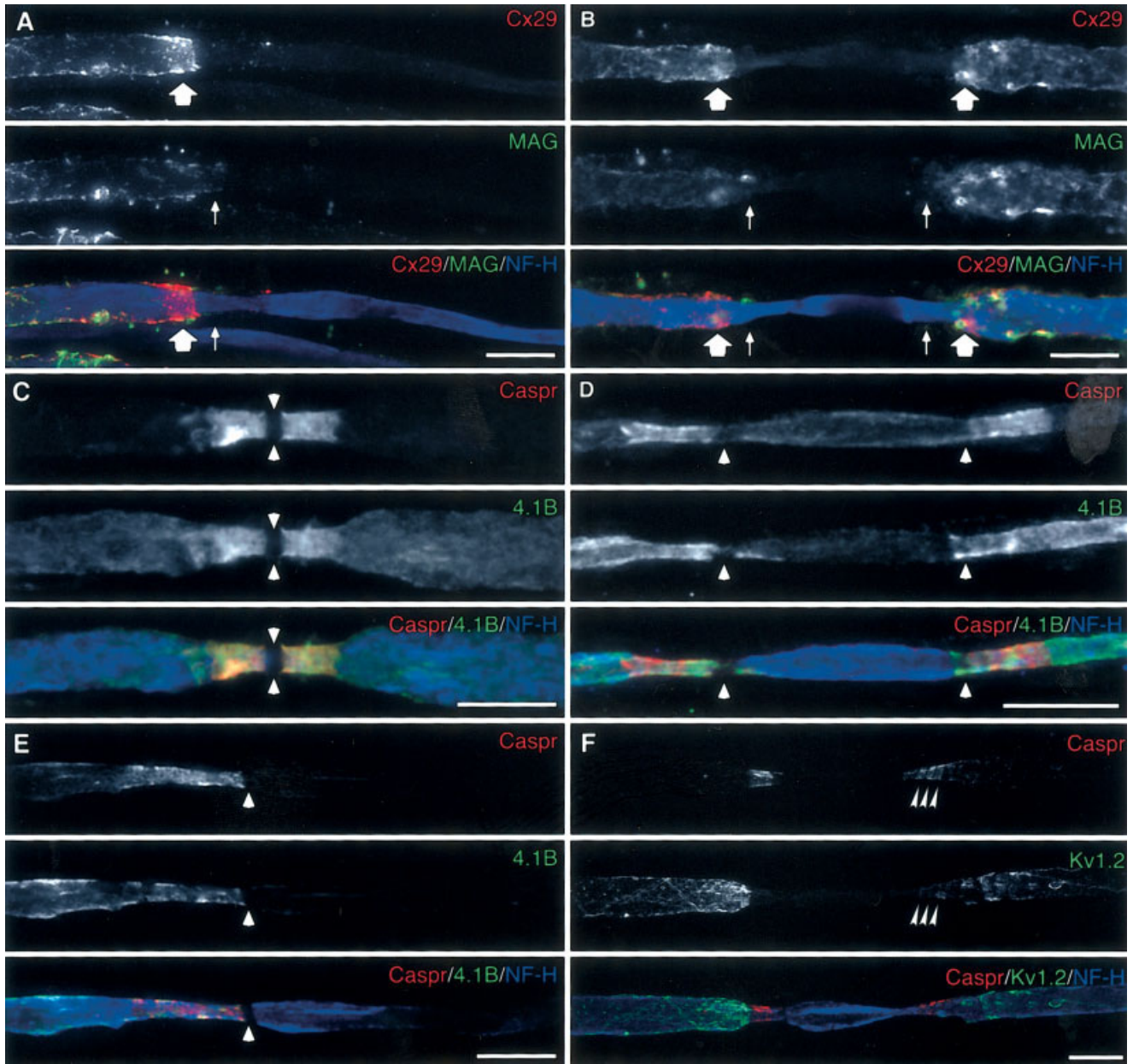


Fig. 6. Paranodal demyelination disrupts paranodal and juxtapanodal components. These are images of teased fibers 5–7 dpi, immunolabeled as indicated; A and F are deconvoluted images. A and E show examples of segmental demyelination; B, D, and F show examples of paranodal demyelination; C shows a normal-appearing node. Symbols as in earlier figures. Note that Cx29 is not localized to

a demyelinated internode (A) or a region of paranodal demyelination (B); that protein 4.1B appears diminished or absent at a normal-appearing node (C), a widened nodal region (D), and a demyelinated internode (E); and that Kv1.2 intercalates between Caspr strands in the paranodal region of an unwound paranode (F). Scale bars = 10 μ m.

jections. This pathological finding has been seen in animals that have been given toxins that cause massive axonal enlargement. Electron microscopy shows that septate-like junctions are translocated toward the internode (Jones and Cavanagh, 1983; Griffin et al., 1987). Based on the colocalization of NF155 and Caspr, it seems likely that septate-like junctions behave similarly in affected fibers after lyssolecithin injections, although we were unable to find examples by electron microscopy. It is

possible that the unwinding of paranodes is related to their formation during development, a matter of some speculation (Pedraza et al., 2001).

These observations bear on the problem of how paranodes appear to prevent Kv1.1/Kv1.2 channels from apposing the Na_v channels at nodes. The loss of septate-like junctions in segmental demyelination results in the redistribution of Kv1.1/Kv1.2 channels (Dugandzija-Novakovic et al., 1995; Novakovic et al., 1996; Rasband et al., 1998).

Just the loss of septate-like junctions alone, without otherwise disrupting the myelin sheath, is sufficient to cause the redistribution of Kv1.1/Kv1.2 channels (Poliak and Peles, 2003). These data indicate that septate-like junctions form a “fence” that separate these K⁺ channels from the node (Rosenbluth, 1988). The intercalation of Kv1.1/Kv1.2 channels into the unwound paranodes is further evidence that septate-like junctions sequester juxtaparanodal proteins.

ACKNOWLEDGMENTS

We thank Drs. Peter Brophy, David Carey, Ed Cooper, Antoine Girault, Masayuki Komada, Virginia Lee, Rock Levinson, Ori Peles, Matt Rasband, and Jim Trimmer for their generous gifts of antibodies.

LITERATURE CITED

- Abe I, Tsjino A, Hara Y, Ichimura H, Ochiai N. 2002. Paranodal demyelination by gradual nerve stretch can be repaired by elongation of internodes. *Acta Neuropathol* 104:505–512.
- Allt G. 1969. Repair of segmental demyelination in peripheral nerves: an electron microscopic study. *Brain* 92:639–646.
- Allt G. 1975. The node of Ranvier in experimental allergic neuritis: an electron microscope study. *J Neurocytol* 4:63–76.
- Altevogt BM, Kleopa KA, Postma FR, Scherer SS, Paul DL. 2002. Cx29 is uniquely distributed within myelinating glial cells of the central and peripheral nervous systems. *J Neurosci* 22:6458–6470.
- Arroyo EJ, Xu Y-T, Zhou L, Messing A, Peles E, Chiu SY, Scherer SS. 1999. Myelinating Schwann cells determine the internodal localization of Kv1.1, Kv1.2, Kvβ2, and Caspr. *J Neurocytol* 28:333–347.
- Arroyo EJ, Xu T, Grinspan J, Lambert S, Levinson SR, Brophy PJ, Peles E, Scherer SS. 2002. Genetic dysmyelination alters the molecular architecture of the nodal region. *J Neurosci* 22:1726–1737.
- Asundi VK, Erdman R, Stahl RC, Carey DJ. 2003. Matrix metalloproteinase-dependent shedding of syndecan-3, a transmembrane heparan sulfate proteoglycan, in Schwann cells. *J Neurosci Res* 73:593–602.
- Ballin RHM, Thomas PK. 1969a. Electron microscope observations on demyelination and remyelination in experimental allergic neuritis. II. Remyelination. *J Neurol Sci* 8:225–237.
- Ballin RHM, Thomas PK. 1969b. Electron microscopic observations on demyelination and remyelination in experimental allergic neuritis. Part I. Demyelination. *J Neurol Sci* 8:1–18.
- Bhat MA, Rios JC, Lu Y, Garcia-Fresco GP, Ching W, St. Martin M, Li JJ, Einheber S, Chesler M, Rosenbluth J, Salzer JL, Bellen HJ. 2001. Axon–glia interactions and the domain organization of myelinated axons requires neurexin IV/Caspr/paranodin. *Neuron* 30:369–383.
- Bonnaud-Toulze EN, Raine CS. 1980. Remodelling during remyelination in the peripheral nervous system. *Neuropathol Appl Neurobiol* 6:279–290.
- Boyle MET, Berglund EO, Murai KK, Weber L, Peles E, Ranscht B. 2001. Contactin orchestrates assembly of the septate-like junctions at the paranode in myelinated peripheral nerve. *Neuron* 30:385–397.

- Dyck PJ, Lais AC, Giannini C, Englestad JK. 1990. Structural alterations of nerve during cuff compression. *Proc Natl Acad Sci U S A* 87:9828–9832.
- Foster RE, Whalen CC, Waxman SG. 1980. Reorganization of the axonal membrane in demyelinated peripheral nerve fibers: morphological evidence. *Science* 210:661–663.
- Girault JA, Peles E. 2002. Development of nodes of Ranvier. *Curr Opin Neurobiol* 12:476–485.
- Gouttebroze L, Carnaud M, Denisenko N, Boutterin M-C, Girault JA. 2003. Syndecan-3 and syndecan-4 are enriched in Schwann cell perinodal processes. *BMC Neurosci* 4:29.
- Griffin JW, Drucker N, Gold BG, Rosenfeld J, Benzzaquen M, Charnas LR, Fahnestock KE, Stocks EA. 1987. Schwann cell proliferation and migration during paranodal demyelination. *J Neurosci* 7:682–299.
- Griffiths I, Klugmann M, Anderson T, Yool D, Thomson C, Schwab MH, Schneider A, Zimmermann F, McCulloch M, Nadon N, Nave KA. 1998. Axonal swellings and degeneration in mice lacking the major proteolipid of myelin. *Science* 280:1610–1613.
- Hall SM. 1973. Some aspects of remyelination after demyelination produced by intraneural injection of lysophosphatidyl choline. *J Cell Sci* 13:461–479.
- Hall SM, Gregson NA. 1971. The in vivo and ultrastructural effects of injection of lysophosphatidyl choline into myelinated peripheral nerve fibers of the adult mouse. *J Cell Sci* 9:767–789.
- Honke K, Hirahara Y, Dupree J, Suzuki K, Popko B, Fukushima K, Fukushima J, Nagasawa T, Yoshida N, Wada Y, Taniguchi N. 2002. Paranodal junction formation and spermatogenesis require sulfoglycolipids. *Proc Natl Acad Sci U S A* 99:4227–4232.
- Jones HB, Cavanagh JB. 1983. Distortions of the nodes of Ranvier from axonal distensions by filamentous masses in hexacarbon intoxication. *J Neurocytol* 12:439–458.
- Kazarinova-Noyes K, Shrager P. 2002. Molecular constituents of the node of Ranvier. *Mol Neurobiol* 26:167–182.
- Komada M, Soriano P. 2002. Beta IV-spectrin regulates sodium channel clustering through ankyrin-G at axon initial segments and nodes of Ranvier. *J Cell Biol* 156:337–348.
- Lambert S, Davis JQ, Bennett V. 1997. Morphogenesis of the node of Ranvier: co-clusters of ankyrin and ankyrin-binding integral proteins define early developmental intermediates. *J Neurosci* 17:7025–7036.
- Lappe-Siefke C, Goebbels S, Gravel M, Nicksch E, Lee J, Braun PE, Griffiths IR, Nave KA. 2003. Disruption of Cnp1 uncouples oligodendroglial functions in axonal support and myelination. *Nat Genet* 33:366–374.
- Lee V, Wu HL, Schlaepfer WW. 1982. Monoclonal antibodies recognized individual neurofilament triplet proteins. *Proc Natl Acad Sci U S A* 79:6089–6092.
- Lee VM-Y, Carden MJ, Schlaepfer WW, Trojanowski JQ. 1987. Monoclonal antibodies distinguish several differentially phosphorylated states of the two largest rat neurofilament subunits (NF-H and NF-M) and demonstrate their existence in the normal nervous system of adult rats. *J Neurosci* 7:3474–3488.
- Li X, Lynn BD, Olson C, Meier C, Davidson KGV, Yasumura T, Rash JE, Nagy JL. 2002. Connexin29 expression, immunocytochemistry and freeze-fracture replica immunogold labelling (FRIL) in sciatic nerve. *Eur J Neurosci* 16:795–806.
- Lubinska L. 1958. 'Intercalated' internodes in nerve fibers. *Nature* 181:957–958.
- Martini R. 2001. The effect of myelinating Schwann cells on axons. *Muscle Nerve* 24:456–466.
- Mata M, Kupina N, Fink DJ. 1992. Phosphorylation-dependent neurofilament epitopes are reduced at the node of Ranvier. *J Neurocytol* 21:199–210.
- Mathis C, Denisenko-Nehrbass N, Girault JA, Borrelli E. 2001. Essential role of oligodendrocytes in the formation and maintenance of central nervous system nodal regions. *Development* 128:4881–4890.
- Melendez-Vasquez CV, Rios JC, Zanazzi G, Lambert S, Bretscher A, Salzer JL. 2001. Nodes of Ranvier form in association with ezrin-radixin-moesin (ERM)-positive Schwann cell processes. *Proc Natl Acad Sci U S A* 98:1235–1240.
- Menegoz M, Gaspar P, Le Bert M, Galvez T, Burgaya F, Palfrey C, Ezan P, Arnos F, Girault J-A. 1997. Paranodin, a glycoprotein of neuronal paranodal membranes. *Neuron* 19:319–331.
- Nguyen T, Arroyo EJ, Scherer SS, Griffin JW. 2004. β , β' -Iminodipropionitrile-induced paranodal demyelination disrupts the molecular organization of nodes. *Neurology* 62:A342–343.
- Novakovic SD, Deerinck TJ, Levinson SR, Shrager P, Ellisman MH. 1996. Clusters of axonal Na⁺ channels adjacent to remyelinating Schwann cells. *J Neurocytol* 25:403–412.
- Ochoa J. 1972. Anatomical changes in peripheral nerves compressed by a pneumatic tourniquet. *J Anat* 113:433–455.
- Ohara R, Yamakawa H, Nakayama M, Ohara O. 2000. Type II brain 4.1 (4.1B/KIAA0987), a member of the protein 4.1 family, is localized to neuronal paranodes. *Brain Res Mol Brain Res* 85:41–52.
- Parra M, Gascard P, Walensky LD, Gimm JA, Blackshaw S, Chan N, Takakuwa Y, Berger T, Lee G, Chasis JA, Snyder SH, Mohandas N, Conboy JG. 2000. Molecular and functional characterization of protein 4.1B, a novel member of the protein 4.1 family with high level, focal expression in brain. *J Biol Chem* 275:3247–3255.
- Pedraza L, Huang JK, Colman DR. 2001. Organizing principles of the axoglial apparatus. *Neuron* 30:335–344.
- Peles E, Nativ M, Lustig M, Grumet M, Martinez R, Plowman GD, Schlessinger J. 1997. Identification of a novel contactin-associated transmembrane receptor with multiple domains implicated in protein-protein interactions. *EMBO J* 16:978–988.
- Poliak S, Peles E. 2003. The local differentiation of myelinated axons at nodes of Ranvier. *Nat Neurosci Rev* 4:968–980.
- Poliak S, Gollan L, Martinez R, Custer A, Einheber S, Salzer JL, Trimmer J, Shrager P, Peles E. 1999. Caspr2, a new member of the neurexin superfamily is localized at the juxtaparanodes of myelinated axons and associates with K⁺ channels. *Neuron* 24:1037–1047.
- Popko B. 2000. Myelin galactolipids: mediators of axon-glia interactions? *Glia* 29:149–153.
- Rasband MN, Shrager P. 2000. Ion channel sequestration in central nervous system axons. *J Physiol* 525:63–73.
- Rasband MN, Trimmer JS. 2001. Subunit composition and novel localization of K⁺ channels in spinal cord. *J Comp Neurol* 429:166–176.
- Rasband M, Trimmer JS, Schwarz TL, Levinson SR, Ellisman MH, Schachner M, Shrager P. 1998. Potassium channel distribution, clustering, and function in remyelinating rat axons. *J Neurosci* 18:36–47.
- Rosenbluth J. 1988. Role of glial cells in the differentiation and function of myelinated axons. *Int J Dev Neurosci* 6:3–24.
- Scherer SS, Xu T, Crino P, Arroyo EJ, Gutmann DH. 2001. Ezrin, radixin, and moesin are components of Schwann cell microvilli. *J Neurosci Res* 65:150–164.
- Scherer SS, Arroyo EJ, Peles E. 2004. Functional organization of the nodes of Ranvier. In: Lazzarini RL, editor. *Myelin biology and disorders*. New York: Elsevier. p 89–116.
- Smith KJ, Hall SM. 1980. Nerve conduction during peripheral demyelination and remyelination. *J Neurol Sci* 48:201–219.
- Suter U, Scherer SS. 2003. Disease mechanisms in inherited neuropathies. *Nat Neurosci Rev* 4:714–726.
- Tait S, Gunn-Moore F, Collinson JM, Huang J, Lubetzki C, Pedraza L, Sherman DL, Colman DR, Brophy PJ. 2000. An oligodendrocyte cell adhesion molecule at the site of assembly of the paranodal axo-glia junction. *J Cell Biol* 150:657–666.
- Vabnick I, Messing A, Chiu SY, Levinson SR, Schachner M, Roder J, Li CM, Novakovic S, Shrager P. 1997. Sodium channel distribution in axons of hypomyelinated and MAG null mutant mice. *J Neurosci Res* 50:321–336.